S-adenosyl-l-homocysteine hydrolase is necessary for aldosterone-induced activity of epithelial Na $^{+}$ channels

James D. Stockand, Shawn Zeltwanger, Hui-Fang Bao, Andrea Becchetti, Roger T. Worrell and Douglas C. Eaton

Am J Physiol Cell Physiol 281:C773-C785, 2001.

AJP - Cell Physiology is dedicated to innovative approaches to the study of cell and molecular physiology. It is published 12 times a year (monthly) by the American Physiological Society, 9650 Rockville Pike, Bethesda MD 20814-3991. ISSN: 0363-6143, ESSN: 1522-1563. Visit our website at http://www.the-aps.org/.

Am J Physiol Cell Physiol
281: C773–C785, 2001.

S-adenosyl-L-homocysteine hydrolase is necessary for aldosterone-induced activity of epithelial Na^+ channels

JAMES D. STOCKAND,[1] SHAWN ZELTWANGER,[2] HUI-FANG BAO,[2]
ANDREA BECCHETTI,[2] ROGER T. WORRELL,[2] AND DOUGLAS C. EATON[2]
[1]*Department of Physiology, University of Texas Health Science Center at San Antonio, San Antonio, Texas 78284; and* [2]*Center for Cell and Molecular Signaling, Department of Physiology, Emory University School of Medicine, Atlanta, Georgia 30322*

Received 2 May 2000; accepted in final form 9 April 2001

Stockand, James D., Shawn Zeltwanger, Hui-Fang Bao, Andrea Becchetti, Roger T. Worrell, and Douglas C. Eaton. *S*-adenosyl-L-homocysteine hydrolase is necessary for aldosterone-induced activity of epithelial Na^+ channels. *Am J Physiol Cell Physiol* 281: C773–C785, 2001.—The A6 cell line was used to study the role of *S*-adenosyl-L-homocysteine hydrolase (SAHHase) in the aldosterone-induced activation of the epithelial Na^+ channel (ENaC). Because aldosterone increases methylation of several different molecules, and because this methylation is associated with increased Na^+ reabsorption, we tested the hypothesis that aldosterone increases the expression and activity of SAHHase protein. The rationale for this work is that general methylation may be promoted by activation of SAHHase, the only enzyme known to metabolize SAH, a potent end-product inhibitor of methylation. Although aldosterone increased SAHHase activity, steroid did not affect SAHHase expression. Antisense *SAHHase* oligonucleotide decreased SAHHase expression and activity. Moreover, this oligonucleotide, as well as a pharmacological inhibitor of SAHHase, decreased aldosterone-induced activity of ENaC via a decrease in ENaC open probability. The kinetics of ENaC in cells treated with antisense plus aldosterone were similar to those reported previously for the channel in the absence of steroid. This is the first report showing that active SAHHase, in part, increases ENaC open probability by reducing the transition rate from open states in response to aldosterone. Thus aldosterone-induced SAHHase activity plays a critical role in shifting ENaC from a gating mode with short open and closed times to one with longer open and closed times.

epithelial sodium channel; hypertension; methylation; *S*-adenosyl-L-methionine; kidney

ALDOSTERONE IS THE PRIMARY HORMONE modulating Na^+ homeostasis. This hormone targets principal cells of the renal collecting duct to increase electrogenic Na^+ reabsorption. This discretionary Na^+ reabsorption establishes a significant osmotic force favoring dependent water reabsorption. Because blood pressure in humans is, in part, determined by plasma volume, aldosterone-mediated reabsorption is an important modulator of blood pressure. Thus it is important to understand the actions of aldosterone at both a systemic and cellular level. While the systemic actions of aldosterone are well established, namely, plasma volume expansion due to increased Na^+ and dependent water reabsorption, the cellular mechanisms of action are enigmatic.

Na^+ reabsorption is a two-step process with active transport across the serosal plasma membrane promoting restrictive diffusion of Na^+ across the luminal plasma membrane. The activity of the luminal cell-entry pathway is rate limiting and increases in response to aldosterone. Serosal Na^+-K^+-ATPases maintain the electrochemical gradient for Na^+ cell entry across the luminal membrane. Luminal entry is through the amiloride-sensitive Na^+-selective ion channel known as epithelial Na^+ channel (ENaC). This 4-pS, amiloride-sensitive Na^+ channel is well characterized (for reviews, see Refs. 5, 11, and 12).

A critical aldosterone-sensitive methylation reaction is thought to be important to steroid-regulated Na^+ reabsorption in some epithelia (24, 29). Aldosterone increases methylation of both lipid and protein through substrate-specific methyltransferases. Transferases transfer a methyl group to a specific protein or lipid target from the methyl donor *S*-adenosyl-methionine. *S*-adenosyl-L-homocysteine (SAH) is one end-product of this reaction; the other is methylated substrate. SAH is a potent negative-feedback inhibitor of most methyltransferases. Thus the enzymes responsible for setting cellular SAH level could play an important role in mediating aldosterone-dependent changes in ENaC activity. Considering this, we suggest that the collective activities of the diverse methyltransferases must depend on the activity of SAH hydrolase (SAHHase; EC 3.3.1.1), the only known enzyme in eukaryotes capable of catabolizing SAH (32). An increase in methyltransferase activities independent of a parallel change in SAHHase activity would lead to cellular accumulation of SAH and subsequent end-product inhibition of further methylation. Moreover, stimulation of SAHHase activity would promote methylation by relieving feed-

Address for reprint requests and other correspondence: J. D. Stockand, Dept. of Physiology, Univ. of Texas Health Science Center at San Antonio, 7703 Floyd Curl Drive, San Antonio, Texas 78284-3900 (E-mail: stockand@UTHSCSA.edu).

The costs of publication of this article were defrayed in part by the payment of page charges. The article must therefore be hereby marked "*advertisement*" in accordance with 18 U.S.C. Section 1734 solely to indicate this fact.

back inhibition, which would not distinguish between transferase types, and could explain the general increase in substrate methylation observed in epithelia upon treatment with aldosterone.

We have previously shown that aldosterone induces SAHHase activity, causing a concomitant increase in substrate methylation (27). While increases in SAHHase activity and methylation are well correlated with increased Na^+ reabsorption, our understanding of the exact effects of SAHHase on the luminal entry pathway, ENaC, are rudimentary. Moreover, it is unclear whether aldosterone increases SAHHase activity by increasing SAHHase protein or by increasing the activity of existing SAHHase protein. The current research demonstrates that aldosterone increases SAHHase activity independent of enzyme expression. Importantly, we show for the first time that active SAHHase is necessary for stabilization of ENaC in the open state (and also in the closed state) with the end result being that the open probability of ENaC increases. This stabilization facilitates Na^+ reabsorption by increasing luminal entry of Na^+. Our results are consistent with ENaC being one final effector of aldosterone-induced SAHHase activity.

MATERIALS AND METHODS

Cell Culture

The amphibian renal epithelial A6 cell line (American Type Culture Collection) was used for all experiments (*passages 71–80*). Cells were maintained in tissue culture by using standard methods described previously (16, 29, 31). Complete but not basic medium was supplemented with 10% (vol/vol) fetal bovine serum and 1.5 μM aldosterone.

For all experiments assessing Na^+ transport, SAHHase activity, and SAHHase protein levels, cells were plated (~1.0×10^6 cells/cm^2) on permeable, 3.8-cm^2 tissue culture inserts (0.02 μM Anopore membrane; Nalge NUNC International) and grown to confluence (~2 wk) in complete medium. This enabled cells to establish polarity and form tight monolayers capable of steroid-sensitive vectorial transport. With these conditions, A6 cells avidly transported Na^+ from luminal to serosal fluids.

For patch-clamp analysis, cells were plated at confluent density on glutaraldehyde-fixed, rat-tail collagen-coated Millipore-CM filters attached to cover the openings (~5–10 mm^2) in the bottom of concave polycarbonate rings (for more detail, refer to Refs. 14, 18, and 20). For at least a week before experimentation, cells were maintained in complete medium to enable this preparation to form a tight, polar epithelium capable of vectorial transport.

To facilitate quantitation of induced Na^+ transport and ENaC activity, we treated confluent monolayers with basic medium for 2 days before experimentation. This treatment established transport at a basal level. All cellular responses to aldosterone were then easily normalized. The current study focused on the aldosterone-signal transduction that culminates in activation of preexisting luminal Na^+ channels (refer to Refs. 5 and 33). Thus all experiments unless indicated otherwise were performed 4 h after addition of aldosterone (1.5 μM) or vehicle (≤0.1% DMSO) to cells previously maintained in basic medium for at least 48 h.

Molecular Biological Methods

Overexpression of SAHHase. Creation of a eukaryotic expression construct containing full-length *Xenopus laevis SAHHase* cDNA has been described (27). This construct, pxSAH, in conjunction with Lipofectamine Plus reagents (Life Technologies), was used to create A6 cells enriched with SAHHase.

Oligonucleotide strategy. SAHHase antisense oligonucleotide (5′-GGACAGTTTGTCAGACATGGTG-3′) was complementary to and spanned the translation start codon (−4 to 18) of *SAHHase* mRNA, whereas sense oligonucleotide (5′-CACCATGTCTGACAAACTGTCC-3′) was homologous to the coding strand. In *X. laevis*, the only sequence with identity to these oligonucleotides as described by a standard nucleotide-nucleotide BLAST search [National Center for Biotechnology Information (NCBI)] was *SAHHase*. Use of these oligonucleotides has been described previously (27). In brief, cells were treated with oligonucleotide (5–10 μM, in basic medium) for 24 h before experimentation. Cells then were treated with aldosterone (1.5 μM) for 4 h in the continued presence of oligonucleotide.

Protein Chemistry

Assay of SAHHase activity. A continuous spectrophotometric enzyme-linked assay, described previously (27), was used to quantify SAHHase activity. SAH hydrolysis results in the formation of adenosine and homocysteine. Our assays were performed in the presence of saturating adenosine deaminase (ADA) activity. Thus we followed the decay of SAH first to adenosine and ultimately to inosine with SAHHase activity being rate limiting.

For these assays, whole A6 cell lysate was extracted by Dounce homogenization of 10^6 cells/ml in 30 mM Tris, 1 mM EDTA, and 1 mM phenylmethylsulfonyl fluoride (PMSF) (pH = 8.0). After cellular debris was cleared, the resulting supernatant was maintained at 4°C and used within 2 h as the source of SAHHase. Enzyme activity was measured in the hydrolytic direction in the following reaction buffer (in mM): 25 KH_2PO_4, 2 $MgCl_2$, and 1 EDTA (pH 7.2). Final reaction volumes of 1 ml contained 698 μl of reaction buffer, 100 μl of 1 mM SAH, 200 μl of whole A6 cell lysate (normalized for protein concentration), and 2 μl of ADA (~5 units; type VIII; Sigma). Reactions were initiated with the addition of lysate, and absorbance changes at a wavelength of 265 nm resulting from SAH metabolism to inosine were recorded with an Ultrospec 3000 spectrophotometer (Pharmacia Biotech). The initial, linear rate of change (1–5 min) was used to calculate activity.

Anti-xSAHHase antisera. A peptide corresponding to residues 413–430 of *X. laevis* SAHHase was synthesized with an amino-terminal cysteine (NH_2-CKQAKYLGLDKEGPFKP-DHKYR-COOH). This peptide was linked to keyhole limpet hemocyanin and used to immunize rabbits (Lofstrand Labs) to create antisera against xSAHHase (AB725). In *X. laevis*, the only polypeptide with identity to the injected antigen as described by a standard protein-protein BLAST search (NCBI) was SAHHase. Rabbits were boosted every 0.5 mo for 3 mo and then placed on production boosts (once a month) for 3 mo with antisera harvested 3–8 mo after initial immunization. For this antisera, a 1:32,000 titer against the immunizing SAHHase antigen was established by ELISA (not shown).

Extraction and immunoblotting. Whole cell lysate was extracted, as previously described (28, 29, 31), with detergent (1% Nonidet P-40) in the following buffer (in mM): 50 Tris·HCl, 76 NaCl, 2 EGTA, and 10% glycerol (pH = 7.4) supplemented with protease inhibitors (1 μM each of PMSF, leupeptin, *N*-tosyl-L-phenylalanine chloromethyl ketone, and N^{ω}-*p*-tosyl-L-lysine chloromethyl ketone). Crude membrane and cytosolic fractions were prepared by differential centrif-

ugation after cells were harvested by sonication in 0.25 M sucrose (10 mM HEPES, pH 7.4). Subsequent to removal of cellular debris, nuclei, and mitochondria, the microsomal fraction (P100) was separated from the cytosol (S100) by centrifugation at 100,000 *g* for 90 min. For whole organ lysates, tissue was obtained from three female frogs (*X. laevis*) maintained on standard diet. Immediately after they were harvested, organs were washed twice with ice-cold PBS and transferred to ice-cold lysis buffer (0.4% sodium deoxycholate, 1% Nonidet P-40, 50 mM EGTA, and 10 mM Tris·HCl, pH 7.4, supplemented with protease inhibitors). Organ homogenates were centrifuged at 5,000 *g* for 10 min and then at 10,000 *g* for 30 min to remove debris.

After the lysate concentration was standardized and sample buffer (which included 20 mM dithiothreitol) was added, samples were boiled (95°C) for 10 min. Sample proteins were then separated by 10% SDS-PAGE, and Western blot analysis was performed using standard procedures. Immunoreactive proteins were visualized using the enhanced chemiluminescence system (Amersham Pharmacia Biotech). Developed Western blots were digitized with the use of a ScanMaker III (Microtex) interfaced with a personal computer running Adobe Photoshop 4.0. Band density was determined by flood analysis with SigmaGel software (Jandel Scientific).

Electrophysiology

Transepithelial electrical measurements. Transepithelial Na^+ reabsorption is reported as transepithelial current calculated under open-circuit conditions from the transepithelial voltage and resistance (corrected for the resistance of the bare filter support). The majority of transport across A6 cells under our experimental conditions is carried by Na^+ with apical entry being limiting. Moreover, all transport is inhibited by the Na^+ channel blocker amiloride. The open-circuit condition, which closely mimics a physiological environment, allows for quantitation of Na^+ reabsorption with adequate cellular material available for subsequent biochemical manipulations.

Transepithelial potentials (PD) and resistances (R) before and after treatment with aldosterone or vehicle were measured with the use of a Millicell Electrical Resistance System with dual Ag-AgCl pellet electrodes (Millipore). Equivalent short-circuit current ($_{eq}I_{sc}$) was then calculated by using Ohm's law, PD = $_{eq}I_{sc}\cdot R$, with current per area reported.

Patch-clamp recording and single-channel analysis. Patch-clamp recording was performed as described previously (14, 18, 20, 30). All experiments were performed at room temperature with patch-clamp pipettes of ~5 MΩ. Pipette and bath solutions were physiological amphibian saline containing (in mM) 100 NaCl, 3.4 KCl, 10 HEPES, 1 $MgCl_2$, and 1 $CaCl_2$ (pH = 7.4). Channel activity was measured with an Axopatch amplifier (Axon Instruments). Current recordings of ENaC were made with no applied pipette potential after gigaohm seals (>20 GΩ) were obtained with the patch electrode on the surface of the A6 cell apical plasma membrane (cell attached). Inward currents (pipette to cytosol) are shown as downward deflections.

Current data were collected using the Axotape program (Axon Instruments). Time and current amplitude data were analyzed with pCLAMP 6 (Axon Instruments). Single-channel unitary current (i) was determined from the best-fit Gaussian distribution of all-point amplitude histograms.

Channel activity within a patch is the product of channel number (N) and open probability (P_o). One method for calculating NP_o is given as

$$NP_o = \sum_{i=0}^{N_A} \frac{it_i}{T} \quad (1)$$

where T is the total recording time, N_A is the observable number of current levels (corresponding to the apparent number of channels) within the patch determined as the highest observable current level, i is the number of channels open, and t_i is the time during which i channels are open. If channels open independently of one another and the exact number of channels in a patch is known, then P_o can be calculated by dividing NP_o by the channel number. The total number of functional channels (N) in the patch was determined by observing the number of peaks detected in all-point amplitude histograms constructed, when possible, from event records of long enough duration to provide 95% confidence of determining the correct N value according to methods we have previously described (14, 20). However, especially in some of the antisense-treated patches, we could not always record long enough to reach a 95% confidence level. Consequently, the values for N in these patches may be underestimated.

Under all conditions, channel activity was calculated before (<10 min after seal formation) ENaC rundown. For all experiments, data were filtered at either 100 or 300 Hz and collected at 2,000 Hz.

Dwell-time analysis of open events was performed with pCLAMP 6 software. After the open times in each patch were measured, events were sorted into logarithmic-scaled bins with 10 bins per decade change in duration according to the method of Sigworth and Sine (25) and plotted as interval histograms. All data for open and closed duration could be fit with a double-exponential function yielding two time constants (open, τ_{O1} and τ_{O2}; closed, τ_{C1} and τ_{C2}).

Materials

Reagents were purchased from either Sigma or Calbiochem unless indicated otherwise. Electrophoresis reagents, materials, and equipment were from Bio-Rad. The Emory University Microchemical Facility synthesized the sense and antisense phosphorothiate oligonucleotides.

Statistical Analysis

Data are presented as means ± SE unless indicated otherwise. Statistical significance for two sets of data was determined with SigmaStat (Jandel Scientific) using Student's t-test. For multiple comparisons, either a one-way ANOVA in conjunction with the Student-Newman-Keuls posttest or, in a few cases, an ANOVA on ranks with a Dunn's posttest was used. For comparison of two proportions or ratios, a z-test with the Yates correction was used. In one case, for multiple proportions, a Chi-square test with Bonferroni's posttest was used. $P \leq 0.05$ was significant.

RESULTS

Characterization of Xenopus laevis SAHHase

Figure 1 shows the characterization of anti-SAHHase antisera AB725. Western blot analysis of whole A6 cell lysate with AB725 antisera identified a protein of 47 kDa. In four experiments, with a typical one shown in Fig. 1*A*, AB725 interaction with the 47-kDa protein was blocked by preabsorption with 0.3 mg/ml antigen, showing this interaction to be specific. Preimmune antisera did not recognize the 47-kDa protein (not shown). Cells transiently transfected with an expression construct containing *SAHHase* cDNA (px-SAH) had 2.2 ± 0.2-fold (n = 10) more SAHHase

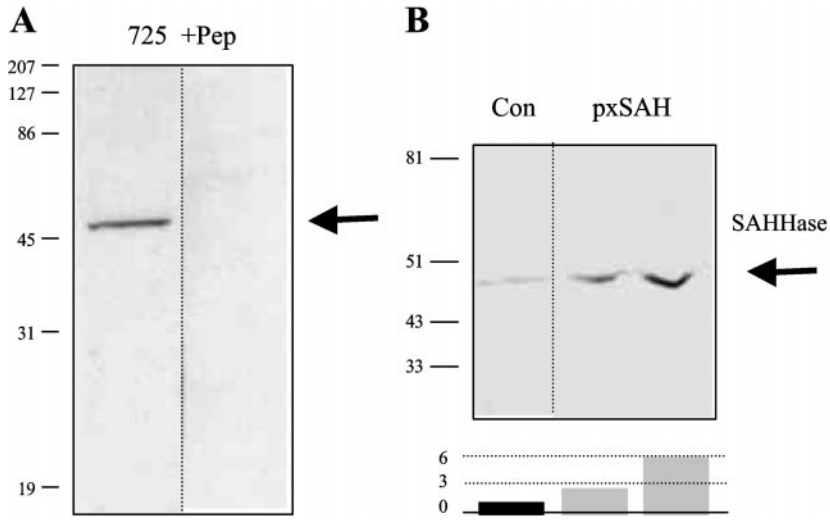

Fig. 1. Characterization of *S*-adenosyl-L-homocysteine hydrolase (SAHHase) in A6 epithelial cells. *A*: typical Western blot ($n = 4$) of whole cell lysate shows that an ~47-kDa protein is specifically identified by AB725 (725). Immunoreactivity of AB725 with this 47-kDa protein was blocked by preabsorption of antibody with antigen (+Pep). *B*: Western blot shows that transfection of A6 cells with pxSAH, an expression vector containing *xSAHHase*, increases the expression of the 47-kDa protein identified by AB725. The first lane contains lysate from control (Con) transfections, and the last two lanes contain lysate from two different groups of A6 cells transfected with pxSAH. All lanes had an equal amount of total protein. Below this typical Western blot ($n = 10$), the optical density (in arbitrary units) is shown for SAHHase in each lysate. Arrows denote SAHHase.

expression compared with control transfectants (Fig. 1*B*). These results are consistent with AB725 antisera being specific for SAHHase protein, which is ~47 kDa under reducing conditions (32).

Figure 2 shows that SAHHase in A6 cells is a cytosolic protein. SAHHase protein, identified with AB725, was 13.3-fold ($n = 4$) enriched in the supernatant (S100) after differential centrifugation, suggesting that this protein is cytosolic (Fig. 2*A*). In contrast, the α-subunits of both ENaC and the Na^+-K^+-ATPase localized to the particulate (P100) fraction (Fig. 2*B*). These latter proteins are well established as intrinsic membrane proteins resident to the apical and basolateral membranes, respectively. The findings that little SAHHase appears in the P100 fraction but that no ENaC or Na^+-K^+-ATPase is detectable in the S100 fraction show successful separation of cytosol from particulate. Aldosterone did not affect localization of SAHHase in A6 cells ($n = 2$, not shown).

The Western blot in Fig. 3 shows the tissue distribution and relative abundance of SAHHase in *X. laevis* ($n = 3$). The blot probed with AB725 (Fig. 3, *top*) is of whole tissue lysates. The black arrow (*top*) marks an immunoreactive protein of ~47 kDa that is competed with antigen (*bottom*). The straight line notes a heavier nonspecific protein identified in both the blot probed with AB725 alone (*top*) and AB725 preabsorbed with antigen (*bottom*). Below the blots is a representation of the optical density (in arbitrary units) of SAHHase in the respective tissues (ordinate is log scale). SAHHase was most abundant in liver followed by oocyte, kidney, and small intestine. Every tissue tested contained SAHHase, a finding consistent with the idea that SAHHase is a ubiquitously expressed enzyme (32).

Aldosterone Increases SAHHase Activity

Figure 4 shows that aldosterone increases SAHHase activity. Figure 4*A* shows the rate of SAH hydrolysis. Lysate (normalized for protein concentration) from A6 cells treated with aldosterone (1.5 μM for 4 h) had higher SAHHase activity compared with lysate prepared from control (untreated) cells. Also shown in Fig. 4*A* is the activity of 1 unit (hydrolytic activity = 1 nM SAH/min at pH 7.2, 37°C) of exogenous rabbit erythrocyte SAHHase (Sigma).

SAHHase activity was determined from the rate of absorbance decay at 265 nm for the first 5 min for both treated and control conditions. The mean SAHHase activity for aldosterone-treated and untreated cells is reported in Fig. 4*B*. Each lysate was assayed at least twice. Aldosterone significantly increased SAHHase activity 2.4 ± 0.4-fold ($n = 4$).

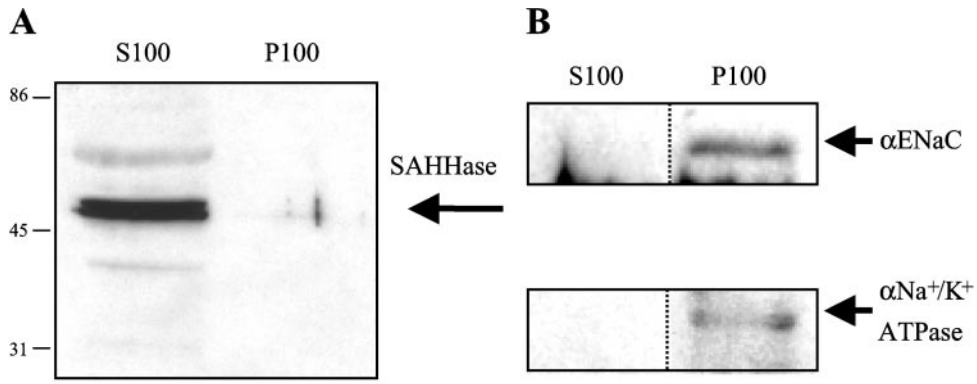

Fig. 2. SAHHase in A6 cells is a cytosolic protein. *A*: Western blot of A6 cell cytosol (S100) and particulate (P100) fraction probed with AB725. SAHHase was 13.3 ± 1.2-fold ($n = 4$) enriched in the cytosolic fraction. *B*: Western blot of A6 cell cytosol and particulate probed with anti-αENaC antibody [*top*; ENaC (epithelial Na^+ channel) is an intrinsic, luminal membrane protein] or anti-αNa^+-K^+-ATPase antibody (*bottom*, this pump is an intrinsic, serosal membrane protein).

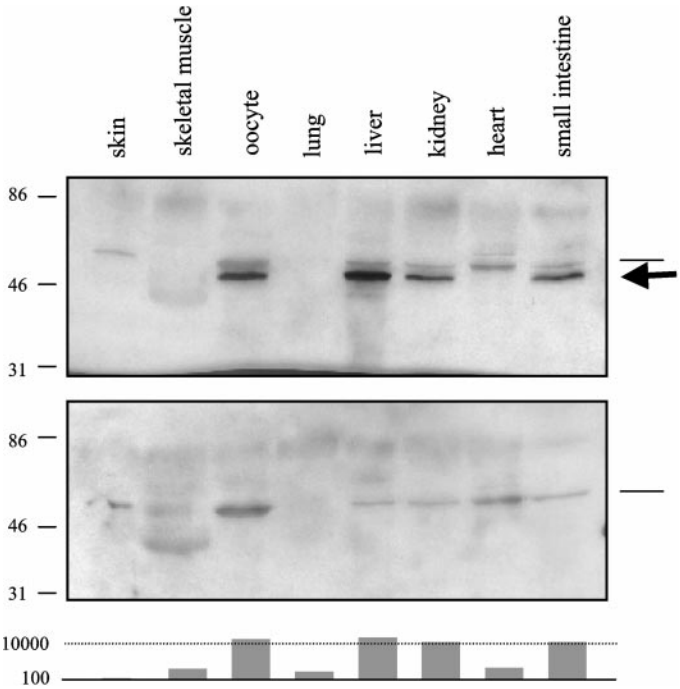

Fig. 3. Tissue distribution of SAHHase in *Xenopus laevis*. *Top blot*: typical blot (n = 3) of whole tissue lysate (tissue types noted). Blot was probed with AB725. An ~47-kDa protein is noted with an arrow, and a distinct heavier protein is noted by a dash. *Bottom blot*: blot probed with AB725 preabsorbed with antigen shows that the 47-kDa protein (SAHHase) but not the heavier protein (dash) specifically interacts with AB725. All lanes contained ~65 μg/well. Bar graph depicts optical density (in arbitrary units) for SAHHase in each tissue type. Liver contained the highest concentration of SAHHase.

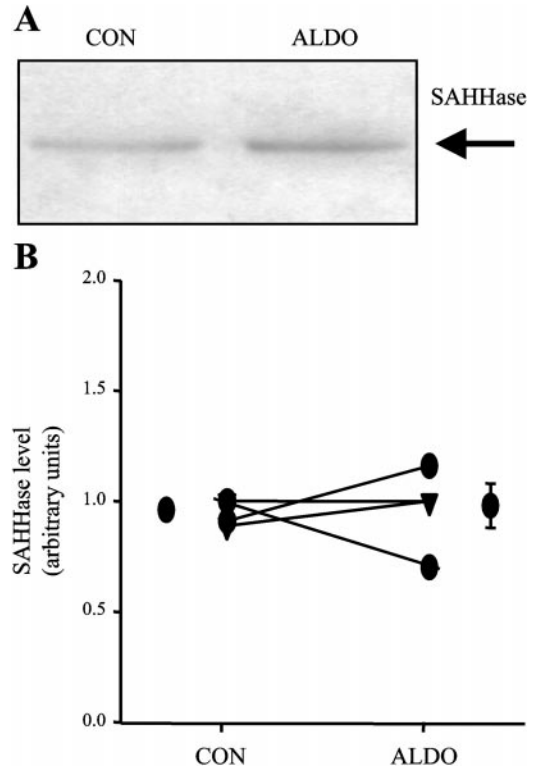

Fig. 5. Aldosterone does not increase SAHHase protein levels. *A*: typical Western blot of whole cell lysate prepared from cells treated with vehicle or aldosterone (1.5 μM) for 4 h probed with AB725 shows that steroid does not increase SAHHase protein levels. The optical density for SAHHase in 4 such experiments is summarized in *B*. The optical density of 0.95 ± 0.03 arbitrary units for SAHHase in control cells was not different from that of 0.97 ± 0.10 for aldosterone-treated cells. Lines connect lysates prepared on the same day.

Results in Fig. 5 demonstrate that the amount of SAHHase protein is not increased by aldosterone. Figure 5*A* shows a typical Western blot (focusing on SAHHase) probed with AB725. This blot contained whole cell lysate extracted from A6 cells that were serum and steroid starved for 48 h and then treated for 4 h with basic medium (control) or medium supplemented with aldosterone (1.5 μM). Four such experiments are summarized in Fig. 5*B*. The optical density (in arbitrary units) of SAHHase in the absence (control) and presence of aldosterone were 0.95 ± 0.03 and 0.97 ± 0.10, respectively, and were not significantly different. These results also show that the apparent size of SAHHase does not change in response to aldosterone as determined by SDS-PAGE under reducing condition.

Functional SAHHase is Necessary for Aldosterone-Induced ENaC Activity

To further investigate the effects of SAHHase activity on Na^+ transport, we examined the effect of an

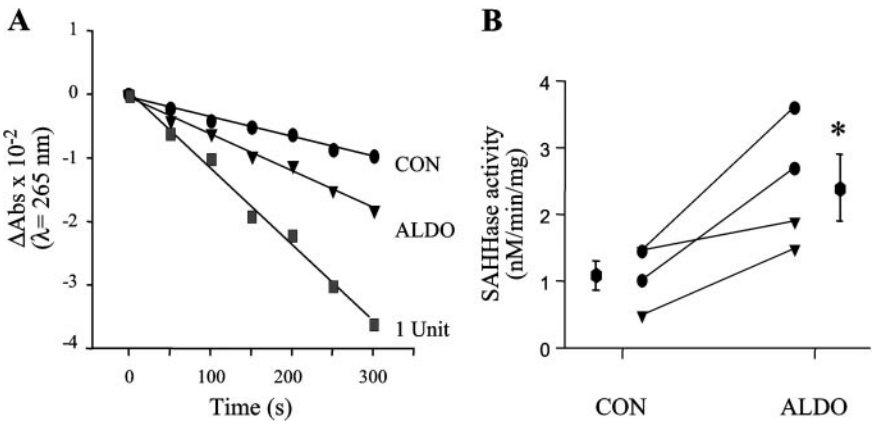

Fig. 4. Aldosterone increases SAHHase activity. *A*: graph depicting absorbance (Abs) at 265 nm shows decay due to metabolism of SAH ultimately into inosine for lysates prepared from control (Con) cells and cells treated with aldosterone (Aldo; 1.5 μM) for 4 h. The faster decay for lysate from aldosterone-treated cells reflects an increased SAHHase activity. The rate of absorbance decay for 1 unit of SAHHase also is shown. The control and aldosterone-treated lysates had an equal amount of total protein. *B*: summary graph of SAHHase activity in cells treated with vehicle (Con) or aldosterone for 4 h. Activity for lysates prepared on the same day are connected by lines. *Cells treated with aldosterone compared with controls had significantly increased SAHHase activity.

SAHHase inhibitor, 3-deazadenosine (DZA), on ENaC. First, paired sets of A6 cells were serum and aldosterone starved for 48 h. One set was additionally treated with 300 μM DZA for 2 h. After this, 1.5 μM aldosterone was added to both sets and ENaC activity was randomly sampled. The aldosterone-sensitive ENaC activity of 0.30 ± 0.19 (mean ± SD, n = 49) in cells pretreated with DZA was significantly lower compared with that of 2.90 ± 0.73 (n = 37) measured in cells treated with aldosterone alone. P_o was also significantly reduced by the action of DZA, from 0.41 ± 0.06 (n = 37) to 0.08 ± 0.03 (n = 49). In eight patches (4 untreated and 4 DZA treated) likely containing only a single channel, the P_o of ENaC in this limited set was somewhat lower than that calculated for ENaC from patches containing larger channel populations, but DZA still significantly reduced P_o from 0.21 ± 0.06 to 0.07 ± 0.01. Representative records and the interval histograms for these patches are shown in Fig. 6. The histograms consist of at least two exponential components reflecting two classes of open events (short and long) and two classes of closed events (short and long). Inhibition of SAHHase with DZA, in addition to reducing P_o, reduced the residency time in all states, both closed and open, short or long. However, residency in long closed states was favored over residency in long open states. This results in the decrease in P_o. Table 1 provides values for the mean durations of the different classes of events and the calculated P_o based on the frequency and duration of the different events.

While DZA inhibition of SAHHase has a profound effect on ENaC kinetics, we worried about the specificity of a pharmacological inhibitor. Thus we used, in addition to DZA, a more specific inhibitor of SAHHase, an oligonucleotide complementary to that area around the translation start codon of *SAHHase* mRNA (see MATERIALS AND METHODS).

Western blot analysis (Fig. 7, *A* and *B*) and an activity graph (Fig. 7*C*) show that SAHHase levels and activity are substantially decreased in cells treated with antisense but not sense *SAHHase* oligonucleotide (5–10 μM for 24 h). A typical Western blot probed with AB725 is shown in Fig. 7*A*. The summary graph in Fig. 7*B* shows that the optical density of SAHHase in the sense group (n = 4) of 4.9 ± 1.7 arbitrary units is significantly greater than that of 1.6 ± 0.5 arbitrary units in the antisense group (n = 7). Sense oligonucle-

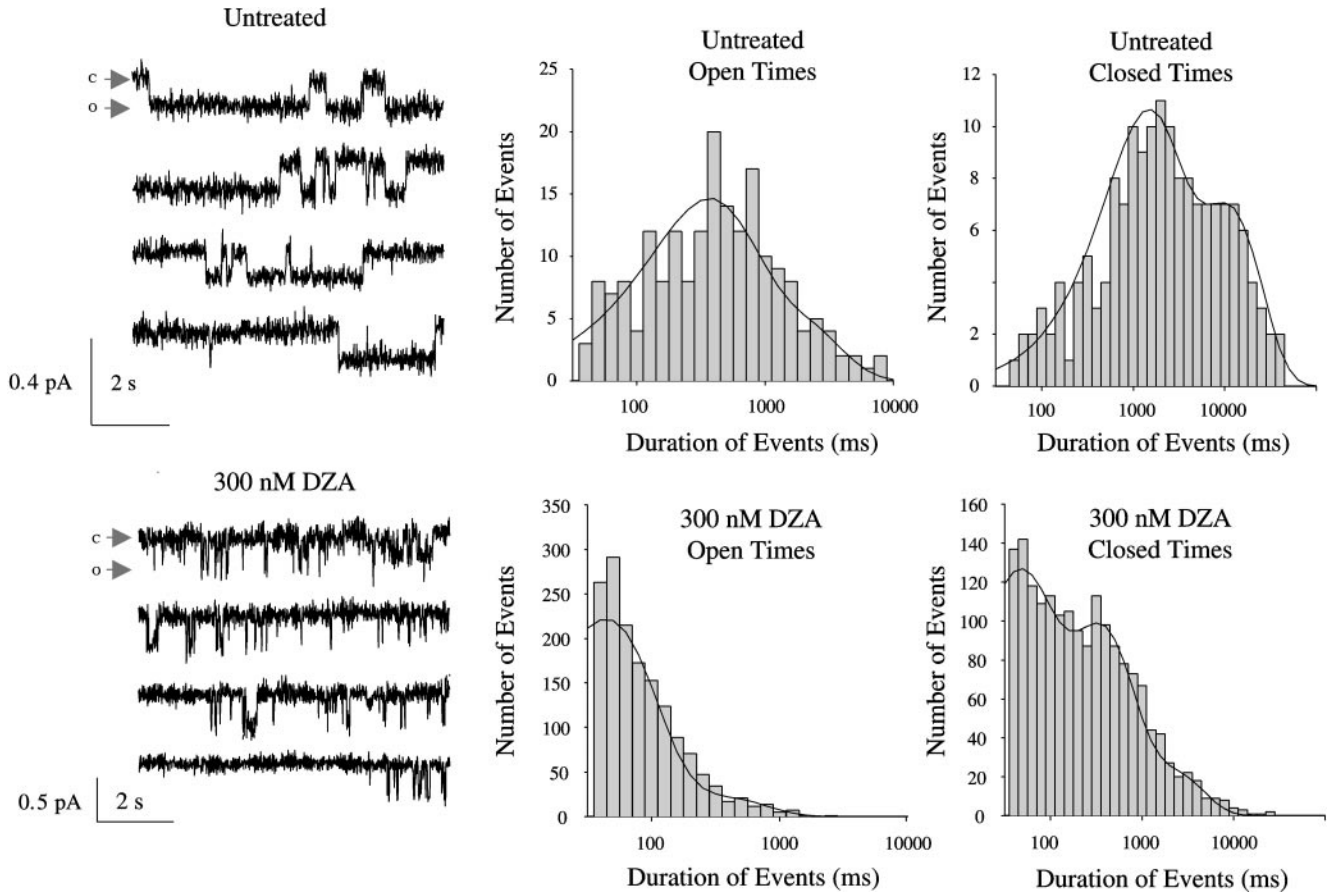

Fig. 6. Effect of the SAHHase inhibitor deazadenosine (DZA) on single-channel kinetics. Representative records (*left*) and interval histograms (*right*) are shown for 8 patches [4 untreated (*top*) and 4 DZA treated (*bottom*)] that were likely to contain only 1 channel. The histograms consist of at least 2 exponential components reflecting 2 classes of open events (short and long) and 2 classes of closed events (short and long). Table 1 provides values for the mean durations of the different classes of events. There are 1,386 events in each untreated histogram and 6,583 events in each DZA histogram.

Table 1. *Effect of the SAHHase inhibitor DZA on ENaC mean open and closed times*

Treatment	n	Mean Durations and Fractional Contributions						
		τ_{O1}, ms	τ_{O2}, ms	Fraction of short open events	τ_{C1}, ms	τ_{C2}, ms	Fraction of short closed events	Calculated P_o
Untreated	4	161 ± 59	1229 ± 418	0.42 ± 0.09	374 ± 167	3,640 ± 1,230	0.35 ± 0.10	0.24 ± 0.04
300 nM DZA	4	26.4 ± 4.6	125 ± 7.0	0.82 ± 0.06	81.1 ± 19.5	1047 ± 271	0.63 ± 0.07	0.11 ± 0.04

Values are means ± SD. Data are from 4 patches (n) with 1 channel and were pooled and fit with 2 exponential functions. *All values for 3-deazadenosine (DZA) are significantly different from control ($P < 0.001$). τ_{O1} and τ_{O2}, mean open times for the short- and long-duration open states; τ_{C1} and τ_{C2}, mean closed times for short- and long-duration closed states; P_o, open probability; SAHHase, *S*-adenosyl-L-homocysteine hydrolase; ENaC, epithelial Na^+ channel.

otide did not itself affect SAHHase levels ($n = 2$) compared with untreated cells.

The graph in Fig. 7*C* shows that *SAHHase* antisense but not sense oligonucleotide also decreases SAHHase activity. The SAHHase activity of 1.5 ± 0.2 nM·min^{-1}·mg^{-1} in the antisense group is significantly less than the 2.5 ± 0.4 nM·min^{-1}·mg^{-1} of the sense group ($n = 5$). Before assay, cells were treated with aldosterone (1.5 μM) for 4 h. Moreover, the SAHHase activity observed in lysate prepared from A6 cells treated with sense oligonucleotide (and aldosterone) was not different from that of control cells (treated with aldosterone alone). As noted previously (27), the sense oligonucleotide does not itself affect SAHHase activity compared with untreated cells.

If SAHHase activity is important for maintaining normal ENaC activity, then antisense treatment should reduce transepithelial Na^+ transport. Figure 8 shows aldosterone-sensitive transepithelial current remaining after pretreatment with sense or antisense oligonucleotide. In the absence of aldosterone, cells treated with either sense (9.6 ± 1.2 μA/cm^2) or antisense oligonucleotide (8.9 ± 1.3 μA/cm^2, $n = 12$) had similar currents, with the current in both groups not differing significantly from that reported previously in the absence of aldosterone with no oligonucleotide (27, 29, 31). Addition of aldosterone to sense-treated cells increased current (to 29.5 ± 1.7 μA/cm^2, $n = 12$) to an extent comparable to that previously reported for addition of aldosterone alone. Conversely, addition of aldosterone to antisense-treated cells produced a significantly smaller increase in current (to 17.4 ± 2.3 μA/cm^2, $n = 12$). Single-channel analysis (see below) suggests that antisense only affects a fraction of the cells. Thus the suppression of aldosterone-sensitive current by antisense may underrepresent the importance of SAHHase to Na^+ reabsorption in this epithelium.

The finding that antisense only affects a fraction of treated cells has been reported previously (13, 17) and is further supported by single-channel measurements from *SAHHase* sense- and antisense-treated cells in which, in this batch of cells, only 8 of 25 cells clearly responded to antisense oligonucleotide. The typical single-channel current traces of Fig. 9, *left*, show ENaC in cell-attached patches on cells treated with either sense (*top left*) or antisense oligonucleotide (*middle* and *bottom left*) for 24 h, in addition to aldosterone for 4 h. The channels from sense-treated cells are not significantly different from those in cells treated with aldosterone alone (Fig. 6 and Table 1). For the group treated with antisense, patches with two distinct types of channel kinetics were observed: one type, which we described as nonresponders (Fig. 9, *middle left*), was similar to the sense-treated group, and the other, which we termed responders (*bottom left*), was distinct from both

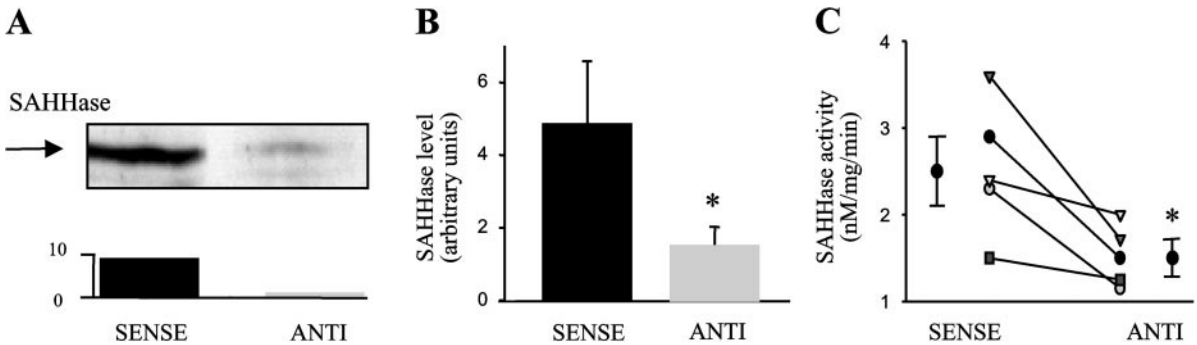

Fig. 7. Antisense *SAHHase* oligonucleotide decreases SAHHase expression and activity. *A*: typical Western blot probed with AB725 of whole cell lysate prepared from A6 cells treated with sense and antisense (Anti) oligonucleotide shows that antisense decreases SAHHase expression. Below the Western blot the optical density of SAHHase is shown for each condition. *B*: summary graph of SAHHase levels from cells treated with sense or antisense oligonucleotide. *The SAHHase level of 1.6 ± 0.5 arbitrary units ($n = 7$) in antisense-treated cells is significantly less than that of 4.9 ± 1.7 arbitrary units in sense-treated cells. *C*: summary graph of SAHHase activity in cells treated with sense or antisense oligonucleotide. *The SAHHase activity of 1.5 ± 0.2 nM·mg^{-1}·min^{-1} ($n = 5$) in antisense-treated cells is significantly (*t*-test) lower than that of 2.5 ± 0.4 nM·mg^{-1}·min^{-1} in sense-treated cells. Lines pair lysates from the same day.

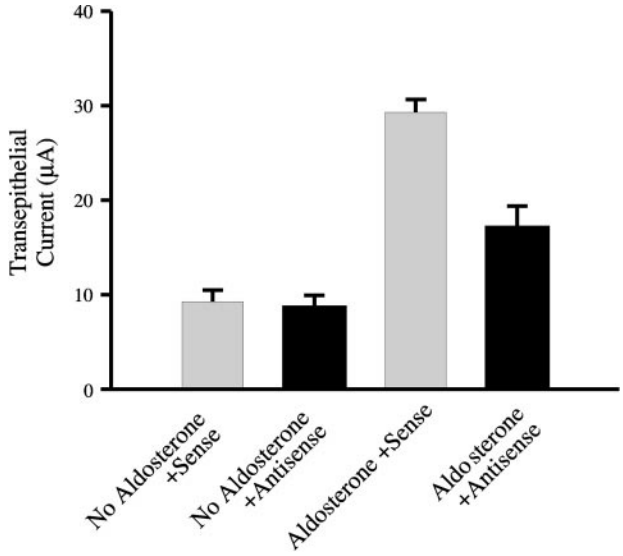

Fig. 8. *SAHHase* antisense oligonucleotide decreases aldosterone-induced transepithelial current. In the absence of aldosterone, cells treated with either sense or antisense oligonucleotides have the same current (9.6 ± 1.23 mA/cm^2 in sense-treated cells vs. 8.9 ± 1.30 mA/cm^2 in antisense-treated cells; n = 12 for each condition). Addition of aldosterone to sense-treated cells increases transepithelial current (to 29.5 ± 1.66 mA/cm^2; n = 12) to an extent comparable to that previously reported for addition of aldosterone alone. Addition of aldosterone to antisense-treated cells produces a significantly smaller increase in current (to 17.4 ± 2.29 mA/cm^2; n = 12).

the sense-treated and nonresponder groups in that the openings were very brief. We categorized a patch as a responder if it had a mean open time <600 ms (>2.7 times smaller than the mean open time for all sense-treated patches). None of the treatments produced any significant change in unitary current measured with no applied potential (−0.29 ± 0.01 pA in sense-treated cells, −0.31 ± 0.03 pA in antisense-treated nonresponding cells, and −0.33 ± 0.04 pA in responding cells).

We examined a total of 109 patches, 50 after treatment with sense oligonucleotide and 59 after treatment with antisense. Of the 50 sense patches, 19 contained at least one ENaC channel, while in the 59 antisense patches, 25 contained at least one ENaC channel. The frequency of observing at least one ENaC in a patch was not significantly different between the sense and antisense groups. ENaC in the 19 patches from sense-treated cells all had mean open times >600 ms and were indistinguishable from those in cells treated with aldosterone alone (Fig. 6 and Table 1; also see Refs. 3 and 20). Conversely, the antisense-treated group consisted of two populations, with 17 nonresponding patches containing ENaC with gating like that of the sense-treated group (mean open time >600 ms) and 8 responding patches containing ENaC with fast gating (mean open time <600 ms). We tested the likelihood of observing such a proportion of differently gating channels in the antisense group when the sense group contained none by using a z-test and found that these two proportions are significantly different ($P <$ 0.001). This finding suggests that antisense *SAHHase* significantly affected at least 32% of the treated cells. Moreover, an examination of the P_o of the three groups indicated no significant difference between the P_o of the sense-treated cells (0.23 ± 0.04) and nonresponding antisense-treated cells (0.23 ± 0.03), but the P_o of the responding antisense-treated cells (0.06 ± 0.01) is significantly different from that of both sense-treated and nonresponding antisense-treated cells. In addition, the distributions of P_o and mean open times of sense-treated and nonresponding antisense-treated cells are normally distributed with overlapping distributions. The distribution of P_o and mean open times of responding antisense-treated cells are also normally distributed but do not significantly overlap either the sense or nonresponding antisense distributions. While ENaC in all patches had two open and two closed states, it was interesting that all channels in a given patch appeared to be affected by oligonucleotide in the same fashion. In other words, ENaC with normal and fast gating were never observed in the same patch. We interpret this as indicating that those cells showing marked changes in channel kinetics were more responsive to antisense oligonucleotides. We have described such a phenomenon before (13).

For each group, Fig. 9 also shows typical dwell-time interval histograms for open and closed events from three to five patches with a statistical probability of containing a single channel: sense (*top right*), nonresponder (*middle right*), and responder (*bottom right*). In all cases, for both closed and open times and sense- and antisense-treated cells, the interval histograms consisted of at least two resolvable exponential components, implying that ENaC had at least four kinetic states, two open and two closed, which we designated C1 (a short-duration closed state), C2 (a long-duration closed state), O1 (a short-duration open state), and O2 (a long-duration closed state) with mean residency times of τ_{C1}, τ_{C2}, τ_{O1}, and τ_{O2}, respectively. Examination of residency times for the three groups indicated that there was no statistical difference between the sense and nonresponder residency times but that responder residency times were significantly different from those for both sense and nonresponder. Therefore, in subsequent results and discussion, we pooled sense and nonresponding cells for comparison with responders. The residency times associated with the four exponential components of the interval histograms are summarized in Table 2. For every component in the responding cells, treatment with antisense oligonucleotide produced a substantial reduction in mean duration. The proportion of long events (both open and closed) also decreased significantly in antisense responding cells.

Despite the fact that the duration of both open and closed events (both short and long) decreased, the overall contribution of closed events increased. Thus we conclude that, like DZA, antisense *SAHHase* decreased aldosterone-sensitive ENaC activity and P_o without significantly changing N. Table 3 shows a summary graph of the activity of ENaC from the sense plus nonresponder and responder groups. The NP_o of 0.47 ±

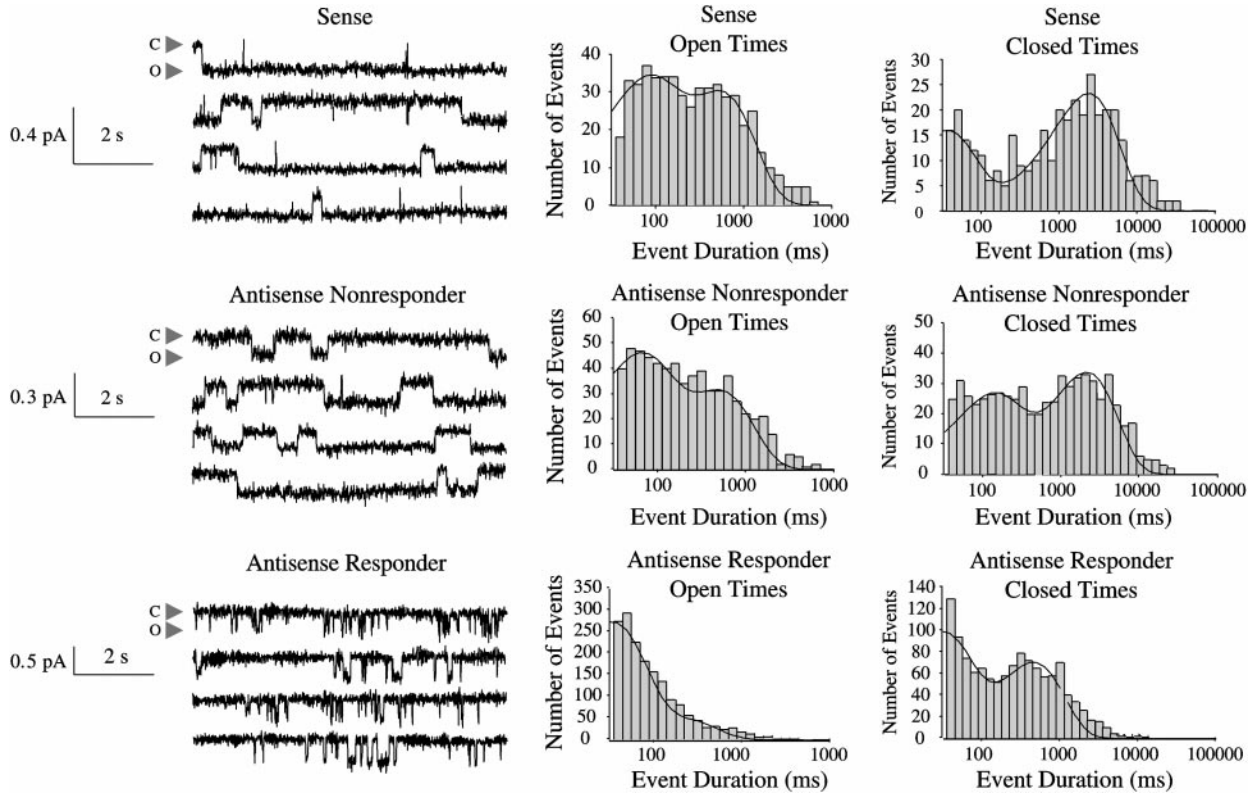

Fig. 9. *SAHHase* antisense oligonucleotide decreases ENaC open and closed times. Left: typical single-channel current traces show ENaC in cell-attached patches on cells treated with either sense (*top*) or antisense oligonucleotide (*middle* and *bottom*) for 24 h, in addition to aldosterone for 4 h. For the group treated with antisense, patches with 2 distinct types of channel kinetics were observed: 1 type, described as nonresponders (*middle*), was similar to the sense-treated group, and the other, termed responders (*bottom*), was distinct from both the sense-treated and nonresponder groups in that the openings were very brief. All patches were cell attached with no applied voltage ($-V_p = 0$ mV). *Right*: for each group, typical dwell-time interval histograms are shown for open and closed events from 3–5 patches with a statistical probability of having only 1 channel. Examination of the residency times for the 3 groups (sense, nonresponders, and responders) indicates that there is no statistical difference between the sense and nonresponder residency times but that responder residency times were significantly different from both sense and nonresponder groups ($P < 0.05$, 1-way ANOVA with Student-Newman-Keuls post hoc test). Sense histograms represent 1,357 events, nonresponder histograms represent 4,742 events, and responder histograms represent 7,518 events (half closed and half open).

0.03 for sense plus nonresponders was significantly greater than that of 0.08 ± 0.01 for responding cells. The number of channels per patch is not significantly different among groups; however, P_o of the responding antisense-treated cells (0.06 ± 0.01, $n = 7$) is significantly less than that of sense plus nonresponding cells (0.23 ± 0.03, $n = 13$).

DISCUSSION

The current study directly assessed the role of SAHHase in the aldosterone-induced activity of the ENaC. Both whole amphibian kidney and A6 cells had significant SAHHase protein expression. While aldosterone increased SAHHase activity, steroid did not affect SAHHase protein expression, suggesting that aldosterone must initiate some posttranslational activation of the enzyme. *SAHHase* antisense oligonucleotide and the inhibitor DZA were used to decrease SAHHase activity. Both DZA and antisense oligonucleotide treatment had profound effects on ENaC: decreasing NP_o, P_o, and mean open and closed times. Interestingly, the kinetics of ENaC in cells treated

Table 2. *Summary of kinetic parameters for ENaC in sense- and antisense-treated cells*

		Mean Durations and Fractional Contributions						
Treatment	n	τ_{O1}, ms	τ_{O2}, ms	Fraction of short open events	τ_{C1}, ms	τ_{C2}, ms	Fraction of short closed events	Calculated P_o
Sense + nonresponders	13	131 ± 36.6	1,287 ± 199	0.54 ± 0.04	415 ± 137	3,815 ± 721	0.37 ± 0.01	0.25 ± 0.04
Antisense responders	7	71.2 ± 35.7	333 ± 119	0.78 ± 0.06	77.9 ± 30.2	1,310 ± 421	0.59 ± 0.01	0.11 ± 0.02

Values are means ± SD; n = no. of patches. *All mean duration values for antisense responders are significantly different from control ($P < 0.001$) except for τ_{O1}, which is different with $P = 0.003$. Values calculated for P_o from event durations and frequencies are not significantly different from the value determined directly from the data records themselves using pCLAMP (see Table 3).

Table 3. *Effect of antisense treatment on channel activity*

Treatment	*n*	NP_o	*N*	P_o
Sense + nonresponders	13	0.47 ± 0.03	1.8 ± 0.98	0.23 ± 0.03
Antisense responders	7	0.08 ± 0.01*	1.2 ± 0.45	0.06 ± 0.01*

Values are means ± SD; *n* = no. of cells. *Significantly different from control group ($P < 0.001$). NP_o, channel activity; *N*, no. of channels.

with aldosterone but in which SAHHase was inhibited with DZA or antisense were similar to those of ENaC in the absence of aldosterone, suggesting that SAHHase is important for aldosterone-induced ENaC activity. Our results as a whole support the hypothesis that aldosterone-induced SAHHase stabilizes all the kinetic states of ENaC in such a manner that P_o increases with a concomitant increase in Na^+ reabsorption.

To understand why the durations of all states of the channel can increase or decrease by approximately the same amount and still produce a change in P_o requires additional consideration. For a channel kinetic scheme containing two open states, O1 and O2, with mean durations of τ_{O1} and τ_{O2}, and two closed states, C1 and C2, with mean durations τ_{C1} and τ_{C2}, the P_o depends on the mean time in each of the four states and the frequency with which these states occur. Therefore, P_o is given as

$$P_o = \frac{f_{O1}\tau_{O1} + f_{O2}\tau_{O2}}{f_{O1}\tau_{O1} + f_{O2}\tau_{O2} + f_{C1}\tau_{C1} + f_{C2}\tau_{C2}} \quad (2)$$

where f_{O1}, f_{O2}, f_{C1}, and f_{C2} are the relative frequencies of the four states O1, O2, C1, and C2, respectively.

Consider one of the responding cells that had a single channel in a patch and in which τ_{O1} = 140 ms, τ_{O2} = 1,257 ms, τ_{C1} = 563 ms, and τ_{C2} = 1,878 ms. The relative frequencies of the different types of events, f_{O1}, f_{O2}, f_{C1}, and f_{C2}, were 0.31, 0.19, 0.25, and 0.25, respectively. With these values, P_o for this channel calculated from *Eq. 1* is 0.32. This value is somewhat higher than the mean values for all sense and nonresponding channels because τ_{C2} is somewhat smaller than the mean value (Table 2). This calculation also illustrates that taking the mean values in Table 2 is not an appropriate way to calculate P_o but, rather, that the individual values for each cell should be used and then a mean calculated P_o determined (as given in Table 2). The question remains, why, if the residency times in all state decreases by approximately the same amount in DZA or antisense responders, should the P_o decrease (rather than stay the same)? Consider a patch on a responding cell that contained a single channel with τ_{O1} = 39.8 ms, τ_{O2} = 188 ms, τ_{C1} = 31 ms, and τ_{C2} = 1,427 ms, all values significantly lower than similar values for untreated or nonresponding channels. The relative frequency of the different types of events, f_{O1}, f_{O2}, f_{C1}, and f_{C2}, were 0.41, 0.09, 0.19, and 0.31, respectively. P_o for this channel as calculated from *Eq. 1* is 0.071. Despite the fact that all the mean durations decreased, the frequency of short openings increased at the expense of long openings and the frequency of long closures increased. The combination of more long closures (even though they are of shorter duration) and fewer long openings is enough to decrease P_o.

Characterization of A6 Cell SAHHase

SAHHase in A6 cells is a cytosolic protein of ~47 KDa under reducing conditions (Figs. 1–4). We believe AB725 to be only the second anti-SAHHase antibody described and the first used to directly show cytosolic localization of SAHHase. The nucleotide sequence of *SAHHase* predicts a protein of ~47 kDa. Aiyar and Hershfield (1), using 8-azido analogs of adenosine and cAMP as photoaffinity reagents in addition to a monoclonal antibody against SAHHase, also identified human placental SAHHase as an ~47-kDa protein. In addition, several investigators have purified SAHHase to homogeneity by standard chromatographic procedures from various species (32). The holoenzyme under native conditions is 189–200 kDa with four (likely homologous) subunits of 47 kDa.

Others have reported (32) that analysis of SAHHase with conditions favoring high resolution reveals two distinct bands of similar density. The apparent doublet at 47 kDa observed in our Western blots of the cytosolic fraction (Fig. 2*A*) is consistent with this earlier finding. What causes the doublet pattern is unclear but may be related to the binding of the SAHHase cofactor NAD^+.

While others have shown SAHHase activity profiles for differing tissues (32), the current study reports tissue distribution of SAHHase using a specific antibody. Figure 3 demonstrates that in *X. laevis,* liver followed by oocyte, kidney, and small intestine has the highest concentration of SAHHase. This is not an unexpected finding. SAHHase activity in mammals is thought to be highest in liver (32). Similarly, the high level of SAHHase that we found in kidney is consistent with previous reports that this tissue has the ability to metabolize a substantial amount of SAH (15, 32). The results in both Figs. 1 and 3 are consistent with the epithelial cells of the distal nephron having significant SAHHase levels.

Activation of SAHHase by Aldosterone

The results of Fig. 4 showing increased SAHHase activity in response to aldosterone are consistent with previous reports that SAHHase activity is increased by adrenal corticosteroids (7, 27). The results in Fig. 5 demonstrate that while activity increases in response to aldosterone, the levels of SAHHase protein in A6 cells are not affected by the steroid. Similarly to other steroids, aldosterone manifests a cellular response through induction of gene expression. Our results are inconsistent with SAHHase being an aldosterone-induced gene product itself, but they indicate that SAHHase appears to be regulated by one. Research that addresses the specific mechanism of increased SAHHase activity in response to aldosterone is pres-

ently being performed. AB725 will be a useful tool in this pursuit.

Active SAHHase is Necessary for Aldosterone-Induced Activation of ENaC

SAHHase expression and activity were decreased with antisense *SAHHase* oligonucleotide (Fig. 7). Activity also was inhibited with DZA (Fig. 6). Two distinct types of ENaC gating were apparent in cells treated with antisense (Fig. 7): one type that had open and closed time constants similar to that of the control sense group (nonresponders), and another type that exhibited very brief openings and closings (responders). Similar to antisense (responders), DZA also resulted in an increase in rapidity of ENaC gating kinetics for all states (Fig. 6). The kinetic parameters and the unitary single-channel current of ENaC in both the sense-treated and nonresponding antisense-treated groups were indistinguishable from the properties of untreated cells (Fig. 6) and similar to values reported previously in A6 cells (2, 3, 14, 18, 20, 34) and in rat renal cortical collecting tubule (CCT) (8, 10, 21). In contrast, the duration of ENaC open and closed events in the responding group was shorter with substantially decreased activity. The kinetic properties of these channels were statistically indistinguishable from those of DZA-treated cells. We have previously used antisense methods to inhibit expression of a variety of proteins (4, 13, 17, 19, 27, 29). In several cases the inhibition of expression is not complete, ranging from extremely effective with undetectable levels of target protein (4) to between 30 and 70% inhibition (13). In the latter case, the inhibition of expression was variable from experiment to experiment. Inhibition of SAHHase expression appears to fall in this variable category. In our single-channel experiments, antisense treatment produced a significant decrease in NP_o, P_o, and mean open and closed times in 36% of the patches we examined. For the number of patches we examined, the upper and lower 95% confidence limits on this percentage are 50.9 and 21.1%. Thus, even if there was not variability in the efficacy of antisense treatment, it is statistically possible that as many as one-half of the cells in our sample were affected.

Our conclusion that antisense affected between one-fifth and one-half of A6 cells and that the gating kinetics of ENaC in these cells were not changed in response to aldosterone (as they were in sense-treated or nonresponding antisense-treated cells) are based on four observations: *1*) antisense decreased Na^+ transport (ENaC is the rate-limiting step in the transcellular pathway); *2*) in the antisense group, channels with both normal and short open times were never seen in the same patch; *3*) the pharmacological inhibitor of SAHHase, DZA, affected ENaC gating kinetics in a manner similar to antisense *SAHHase*; and *4*) the proportional decrease in SAHHase activity, SAHHase level, P_o, and transepithelial current produced by antisense or DZA was not significantly different. The fractional reduction in each of these values is presented in Table 4. As expected, DZA produces the largest inhibition, since it affects all cells and the effect of DZA on transepithelial current and P_o are close to the same (0.20 ± 0.01 vs. 0.17 ± 0.04 of control, respectively). The effect of antisense on SAHHase activity and transepithelial current is also similar (0.60 ± 0.13 vs. 0.59 ± 0.08 of control, respectively) and the effect of antisense on the P_o of responding cells (0.28 ± 0.05 of control) is comparable to the change in transepithelial current and SAHHase activity after we correct for the fact that only 36% of cells are represented in the responder category (which would produce a reduction in current to ~0.74 of control). The reduction in apparent amount of SAHHase protein (to 0.33 ± 0.15 of control) is larger than expected compared with other measures but is not statistically different. Given the large differences in the types of experiments, the fractional reductions are quite similar.

Table 4. *Relative magnitude of the effect of antisense oligonucleotide or DZA on measures of sodium transport*

Experiment	Fraction of Control
Reduction of SAHHase activity by antisense	0.60 ± 0.13
Reduction of SAHHase protein by antisense	0.33 ± 0.15
Reduction of P_o in responding cells	0.28 ± 0.05
Reduction of transepithelial current by antisense	0.59 ± 0.08
Reduction of P_o by DZA	0.20 ± 0.01
Reduction of transepithelial current by DZA	0.17 ± 0.04

Values are means ± SE.

It is possible that the difference between the effect of antisense on transepithelial current and its effect on P_o could be due to our underestimating the number of cells that respond to antisense. Our use of a 600-ms cutoff was somewhat arbitrary (based on normal distributions of mean open time and P_o). In fact, though there was no statistical difference in the mean values for the sense-treated cells and the nonresponding cells, five of seven of the individual values obtained from patches with apparently only a single channel are less than all values for sense-treated cells. Thus there may be some partial effect of the antisense oligonucleotides that would be expected to reduce the transepithelial current below levels expected from a simple extrapolation of the P_o of ENaC in cells we categorized as responders.

As mentioned earlier, all ENaC openings in A6 cells were described by two types of open and closed events with mean open time constants τ_{O1} and τ_{O2} and τ_{C1} and τ_{C2} (Figs. 7 and 9). Kemendy et al. (14) in A6 cells and Palmer and Frindt (22) in CCT principal cells also showed that ENaC has two open and closed states. All of our findings are consistent with aldosterone-activated SAHHase stabilizing all of these states. Antisense *SAHHase* reduced the open time constants of ENaC, leading to the appearance of the characteristic gating associated with the responding cell type, but antisense oligonucleotide did not affect single-channel unitary current. These results demonstrate that while SAHHase is important to ENaC gating, this enzyme

does not play a role in determining ENaC conductance. Because antisense failed to affect unitary conductance, the decrease in both τ_{O1} and τ_{O2} relative to changes in τ_{C1} and τ_{C2} in response to antisense must produce, in a large part, the decrease in ENaC activity shown in Figs. 8 and 11.

The open time constants for ENaC for sense-treated and nonresponding cells are consistent with those previously reported for ENaC in A6 cells treated with aldosterone for 6 h (14, 28, 31). In this earlier report, both the longer and shorter open time constants were greater in the presence of aldosterone compared with those in the absence of steroid. In fact, the longer open time constant was 30-fold lower in the absence of aldosterone. The results of the present study and this earlier finding are consistent with the hypothesis that aldosterone via activation of SAHHase stabilizes ENaC open states, resulting in increased P_o.

Interestingly, Palmer and Frindt (22) have reported three types of gating kinetics resulting in distinct P_o for ENaC from rat CCT: *1*) low P_o (τ_{O1} = 24 ms and τ_{O2} = 123 ms), *2*) intermediate P_o (τ_{O1} = 95 ms and τ_{O2} = 761 ms), and *3*) high P_o (τ_{O1} = 82 ms and τ_{O2} = 1,810 ms). In this study, the authors suggested that these ENaCs are identical in structure but are merely in different gating modes. This raises the question, what determines the gating mode of ENaCs? Our results suggest that SAHHase activity, in part, plays a role in controlling ENaC gating.

Open times of the low-P_o channel described by Palmer and Frindt (22) are similar to those of ENaC in antisense-responding or DZA-treated cells in the present study, and the open times of the high-P_o channel are similar to those for channels in our sense-treated and nonresponding cells. We believe both studies are consistent with the idea that aldosterone (possibly via SAHHase) plays a role in ENaC gating. Palmer and Frindt used whole animal manipulations (a low-Na^+ diet) to produce high levels of circulating aldosterone. All three types of ENaC gating kinetics thus were observed in animals with high aldosterone levels. Because patches containing only single channels were analyzed in Palmer and Frindt's study, it was unclear whether ENaC with distinct gating kinetics coexisted in the same cell. We have never observed and are not aware of any other study showing multiple types of gating kinetics for ENaCs within the same patch. In the context of our results showing that aldosterone via SAHHase stabilizes ENaC channel states, a possible explanation reconciling Palmer and Frindt's results with ours is that cells containing low P_o-type channels simply did not respond to aldosterone. In whole animal manipulations, any one of a number of reasons could result in a set of cells failing to respond to aldosterone. Alternatively, all three of the channel types reported by Palmer and Frindt may have existed in both our sense- and antisense-treated cells and we missed them due to sample size. However, we do not believe this latter explanation to be true because *1*) there was a significant difference between the proportion of ENaC with decreased open time constants vs. ENaC with longer open times in the antisense- compared with sense-treated cells; in fact, we never saw the low P_o-type channel in the sense-treated cells; *2*) in the antisense group, a low P_o- and higher P_o-type channel were never observed in the same patch; and *3*) the decrease in transepithelial Na^+ reabsorption across antisense-treated cells is consistent with a change in ENaC activity. Active SAHHase may be a trigger that converts the channels from the low-P_o gating mode to that of the higher P_o variety.

While our results support the idea that aldosterone-sensitive increases in ENaC activity in amphibian renal epithelia are, at least partially, linked to steroid actions on SAHHase activity, the cellular signaling cascade linking SAHHase activity to changes in ENaC kinetics is not completely clear. However, we and others have shown that the primary effect of SAHHase is to metabolize SAH and, thus, prevent it from becoming a rate-limiting inhibitor of methyltransferases (27, 32). We have also demonstrated that the methyltransferase important for ENaC regulation is an isoprenylcysteine carboxylmethyltransferase (29) that possibly methylates a small G protein, K-Ras2A (2, 31). Aldosterone induces production of K-Ras2A, and subsequent methylation enables K-Ras2A to become active in response to GTP binding (2, 26, 31). Activated K-Ras2A increases the P_o of ENaC (3) by an as yet unknown mechanism. On the other hand, while some of the elements downstream of SAHHase are known, how aldosterone increases SAHHase activity also remains to be determined. Because there is no change in SAHHase protein amount, aldosterone likely increases SAHHase activity by promoting posttranslational modification of SAHHase.

Other investigators have been unable to show an effect of methylation on ENaC in rat CCT principal cells (9). This may only mean that methylation is necessary but is not the rate-limiting step for activation of ENaC in rat epithelial cells. Nonetheless, the central importance of this pathway for controlling ENaC in all epithelial tissue capable of Na^+ absorption remains unclear. However, in diverse cells, including A6 cells, toad urinary bladder cells and possibly bovine distal collecting duct cells, methylation and, thus, SAHHase appears to play a role in regulating Na^+ transport via ENaC (reviewed in Refs. 24 and 29).

The current results describe a novel anti-SAHHase antibody. This is the first time an anti-SAHHase antibody has been used to profile tissue distribution and cellular localization of SAHHase. Our report that SAHHase activity is elevated in A6 cells treated with adrenal steroid is consistent with previously published results (7, 23, 27). While aldosterone enhanced activity, steroid failed to alter SAHHase protein levels, proving that aldosterone does not induce the expression of SAHHase but may lead to posttranslational processing of this protein. Experiments utilizing antisense *SAHHase* oligonucleotide showed that under conditions where SAHHase protein levels and activity are depressed, a distinct type of ENaC gating characterized by markedly reduced channel open times be-

comes apparent. Similar results were observed when DZA was used to inhibit SAHHase. The openings and closings for all ENaC in our study could be described by two time constants. This finding suggests that active SAHHase is necessary for stable channel openings and that inhibition of SAHHase blocks the ability of aldosterone to maintain Na^+ channels with high open probability. We propose that to increase Na^+ reabsorption, aldosterone via SAHHase stabilizes ENaC in all kinetic states but that open states are favored enough to produce an increase in open probability.

We thank B. J. Duke for excellent technical support.

This research was supported by National Institute of Diabetes and Digestive and Kidney Diseases Grants DK-09729 (to J. D. Stockand) and DK-37963 (to D. C. Eaton).

REFERENCES

1. **Aiyar VN and Hershfield MS.** Covalent labelling of ligand binding sites of human placental *S*-adenosylhomocysteine hydrolase with 8-azido derivatives of adenosine and cyclic AMP. *Biochem J* 232: 643–650, 1985.
2. **Al Baldawi NF, Stockand JD, Al Khalili OK, Yue G, and Eaton DC.** Aldosterone induces ras methylation in A6 epithelia. *Am J Physiol Cell Physiol* 279: C429–C439, 2000.
3. **Becchetti A, Kemendy AE, Stockand JD, Sariban-Sohraby S, and Eaton DC.** Methylation increases the open probability of the epithelial sodium channel in A6 epithelia. *J Biol Chem* 275: 16550–16559, 2000.
4. **Denson DD, Worrell RT, Middleton P, and Eaton DC.** Ca^{2+} sensitivity of BK channels in GH3 cells involves cytosolic phospholipase A2. *Am J Physiol Cell Physiol* 276: C201–C209, 1999.
5. **Eaton DC, Becchetti A, Ma H, and Ling BN.** Renal sodium channels: regulation and single channel properties. *Kidney Int* 48: 941–949, 1995.
7. **Finkelstein JD and Harris B.** Methionine metabolism in mammals: synthesis of *S*-adenosylhomocysteine in rat tissues. *Arch Biochem Biophys* 159: 160–165, 1973.
8. **Frindt G, Masilamani S, Knepper MA, and Palmer LG.** Activation of epithelial Na channels during short-term Na deprivation. *Am J Physiol Renal Physiol* 280: F112–F118, 2001.
9. **Frindt G and Palmer LG.** Regulation of Na channels in the rat cortical collecting tubule: effects of cAMP and methyl donors. *Am J Physiol Renal Fluid Electrolyte Physiol* 271: F1086–F1092, 1996.
10. **Frindt G, Palmer LG, and Windhager EE.** Feedback regulation of Na channels in rat CCT. IV. Mediation by activation of protein kinase C. *Am J Physiol Renal Fluid Electrolyte Physiol* 270: F371–F376, 1996.
11. **Garty H.** Regulation of the epithelial Na^+ channel by aldosterone: open questions and emerging answers. *Kidney Int* 57: 1270–1276, 2000.
12. **Garty H and Palmer LG.** Epithelial sodium channels: function, structure, and regulation. *Physiol Rev* 77: 359–396, 1997.
13. **Jain L, Chen XJ, Malik B, Al-Khalili OK, and Eaton DC.** Antisense oligonucleotides against the α-subunit of ENaC decrease lung epithelial cation-channel activity. *Am J Physiol Lung Cell Mol Physiol* 276: L1046–L1051, 1999.
14. **Kemendy AE, Kleyman TR, and Eaton DC.** Aldosterone alters the open probability of amiloride-blockable sodium channels in A6 epithelia. *Am J Physiol Cell Physiol* 263: C825–C837, 1992.
15. **Kloor D, Kurz J, Fuchs S, Faust B, and Osswald H.** *S*-adenosylhomocysteine-hydrolase from bovine kidney: enzymatic and binding properties. *Renal Physiol Biochem* 19: 100–108, 1996.
16. **Ling BN, Kemendy AE, Kokko KE, Hinton CF, Marunaka Y, and Eaton DC.** Regulation of the amiloride-blockable sodium channel from epithelial tissue. *Mol Cell Biochem* 99: 141–150, 1990.
17. **Ling BN, Zuckerman JB, Lin C, Harte BJ, McNulty KA, Smith PR, Gomez LM, Worrell RT, Eaton DC, and Kleyman TR.** Expression of the cystic fibrosis phenotype in a renal amphibian epithelial cell line. *J Biol Chem* 272: 594–600, 1997.
18. **Ma H and Ling BN.** Luminal adenosine receptors regulate amiloride-sensitive, Na^+ channels in A6 distal nephron cells. *Am J Physiol Renal Fluid Electrolyte Physiol* 270: F798–F805, 1996.
19. **Ma H, Matsunaga H, Li B, Schieffer B, Marrero MB, and Ling BN.** Ca^{2+} channel activation by platelet-derived growth factor-induced tyrosine phosphorylation and Ras guanine triphosphate-binding proteins in rat glomerular mesangial cells. *J Clin Invest* 97: 2332–2341, 1996.
20. **Marunaka Y and Eaton DC.** Effects of vasopressin and cAMP on single amiloride-blockable Na channels. *Am J Physiol Cell Physiol* 260: C1071–C1084, 1991.
21. **Palmer LG and Frindt G.** Amiloride-sensitive Na channels from the apical membrane of the rat cortical collecting tubule. *Proc Natl Acad Sci USA* 83: 2767–2770, 1986.
22. **Palmer LG and Frindt G.** Gating of Na channels in the rat cortical collecting tubule: effects of voltage and membrane stretch. *J Gen Physiol* 107: 35–45, 1996.
23. **Radomski N, Kaufmann C, and Dreyer C.** Nuclear accumulation of *S*-adenosylhomocysteine hydrolase in transcriptionally active cells during development of *Xenopus laevis*. *Mol Biol Cell* 10: 4283–4298, 1999.
24. **Sariban-Sohraby S and Fisher RS.** Guanine nucleotide-dependent carboxymethylation: a pathway for aldosterone modulation of apical Na^+ permeability in epithelia. *Kidney Int* 48: 965–969, 1995.
25. **Sigworth FJ and Sine SM.** Data transformations for improved display and fitting of single-channel dwell time histograms. *Biophys J* 52: 1047–1054, 1987.
26. **Spindler B, Mastroberardino L, Custer M, and Verrey F.** Characterization of early aldosterone-induced RNAs identified in A6 kidney epithelia. *Pflügers Arch* 434: 323–331, 1997.
27. **Stockand JD, Al Baldawi NF, Al Khalili OK, Worrell RT, and Eaton DC.** *S*-adenosyl-L-homocysteine hydrolase regulates aldosterone-induced Na^+ transport. *J Biol Chem* 274: 3842–3850, 1999.
28. **Stockand JD, Bao HF, Schenck J, Malik B, Middleton P, Schlanger LE, and Eaton DC.** Differential effects of protein kinase C on the levels of epithelial Na^+ channel subunit proteins. *J Biol Chem* 275: 25760–25765, 2000.
29. **Stockand JD, Edinger RS, Al-Baldawi NF, Sariban-Sohraby S, Al-Khalili OK, Eaton DC, and Johnson JP.** Isoprenylcysteine-*O*-carboxyl methyltransferase regulates aldosterone-sensitive Na^+ reabsorption. *J Biol Chem* 274: 26912–26916, 1999.
30. **Stockand JD and Sansom SC.** Role of large Ca^{2+}-activated K^+ channels in regulation of mesangial contraction by nitroprusside and ANP. *Am J Physiol Cell Physiol* 270: C1773–C1779, 1996.
31. **Stockand JD, Spier B, Worrell RT, Yue G, Al-Baldawi NF, and Eaton DC.** Regulation of Na^+ reabsorption by the aldosterone-induced small G protein K-Ras2A. *J Biol Chem* 274: 35449–35455, 1999.
32. **Ueland PM.** Pharmacological and biochemical aspects of *S*-adenosylhomocysteine and *S*-adenosylhomocysteine hydrolase. *Pharmacol Rev* 34: 223–253, 1982.
33. **Verrey F.** Transcriptional control of sodium transport in tight epithelial by adrenal steroids. *J Membr Biol* 144: 93–110, 1995.
34. **Yue G, Edinger RS, Bao HF, Johnson JP, and Eaton DC.** The effect of rapamycin on single ENaC channel activity and phosphorylation in A6 cells. *Am J Physiol Cell Physiol* 279: C81–C88, 2000.